

## Research Article

# Narrowband AM Interference Cancellation for Broadband Multicarrier Systems

Dieter Van Welden and Heidi Steendam

*Department of Telecommunications and Information Processing, Ghent University,  
Sint-Pietersnieuwstraat 41, 9000 Gent, Belgium*

Correspondence should be addressed to Dieter Van Welden, [dmvwelde@telin.ugent.be](mailto:dmvwelde@telin.ugent.be)

Received 31 May 2007; Revised 12 December 2007; Accepted 4 February 2008

Recommended by Ryuji Kohno

We consider an overlay system where narrowband AM signals interfere with a broadband multicarrier system. To reduce the effect of the AM narrowband interference on the multicarrier system, we propose a low-complexity algorithm to estimate the AM narrowband interference. Analytical expressions for the performance of this estimator are derived and verified with simulations. The performance of this estimator, however, degrades when the number of interferers increases. To improve the algorithm, we adapt it such that the interferers are estimated in a successive way. The proposed estimators are able to produce accurate estimates of the frequencies, and track the time-varying amplitudes of the AM signals. The estimators can reduce the power of the AM signal to a level that is approximately 20 dB lower than the multicarrier power, independently of the AM signal power.

Copyright © 2008 D. Van Welden and H. Steendam. This is an open access article distributed under the Creative Commons Attribution License, which permits unrestricted use, distribution, and reproduction in any medium, provided the original work is properly cited.

## 1. INTRODUCTION

In aeronautical communication, nowadays narrowband VHF signals are used for communication between the ground station and the air carriers. Most of these VHF signals consist of analog dual-sideband amplitude modulated (DSB-AM) signals for voice communication. However, as the air traffic is constantly increasing, the available bandwidth is fixed, and the used VHF signals are bandwidth inefficient, it is expected that the available bandwidth resources will be insufficient by the year 2015. Hence, an alternative bandwidth efficient communication system has to be found. A technique that combines a high bandwidth efficiency with a high flexibility and immunity to dispersive channels is multicarrier (MC) modulation [1]. The MC technique has been proposed and/or standardized for various applications, like, for example, ADSL [2], wireless LAN (hiperlan, IEEE 802.11) [3, 4], digital audio, and video broadcasting [5, 6], and so forth.

In the B-VHF project [7, 8], a broadband multicarrier system was proposed for the 118–138 MHz aeronautical band. In this cellular-based system, the overlay B-VHF system has to coexist with the narrowband VHF legacy systems. The B-VHF system is aware of the presence of the legacy signals and adapts its signal to keep the interference from the B-

VHF system to the legacy as small as possible and vice versa. We can consider two types of interference from the legacy systems to the B-VHF system: intracell interference, coming from legacy systems that are located in the same cell as the B-VHF system, and intercell interference, coming from legacy systems from neighboring cells. Intracell interference is reduced by not using parts of the frequency band of the B-VHF system where (possibly) narrowband legacy VHF signals reside. This frequency gap in the B-VHF spectrum not only copes with the interference from the legacy systems to the B-VHF system but also reduces the disturbance from the B-VHF system on the legacy systems. In contrast with interference within the B-VHF cell, the B-VHF system does not provide a frequency gap on frequencies used by legacy systems from other cells. Although the intercell interference is typically weaker than intracell interference, the intercell interference can strongly reduce the B-VHF performance [9].

In the literature, several techniques were considered to reduce the effect of the AM interferers on the B-VHF performance. In [10], the authors use time domain windowing to reduce the spectral width of a B-VHF carrier to reduce the out-of-band radiation from the B-VHF system to the legacy systems. However, this technique also has the beneficial effect that the interference of the legacy system on the B-VHF

system will be reduced as the spectral leakage is reduced: less B-VHF carriers will be affected by the interference. However, the performance gain that can be achieved in the B-VHF system with this technique is rather small. An interference cancellation technique that estimates and subtracts the legacy signals from the received signal is considered in [10]. The technique uses the frequency gaps, where no B-VHF signal is present, to estimate the interferers in the frequency domain. However, as this technique needs the presence of the frequency gap, it is not able to eliminate interferers from other cells. In this paper, we propose a novel algorithm to estimate and cancel narrowband AM interferers from within the B-VHF cell and from neighboring cells by using a low-complexity time domain approach. The work in this paper is an extension from our work in [11].

## 2. SYSTEM MODEL

The received signal  $r(t)$  at the receiver of the multicarrier system consists of the useful multicarrier signal  $r_{MC}(t)$ , the signal  $r_{AM}(t)$  caused by the AM interferers, and noise  $w(t)$ :

$$r(t) = r_{MC}(t) + r_{AM}(t) + w(t). \quad (1)$$

We assume that the bandwidth of the AM narrowband signal is small as compared to the coherence bandwidth of the channel, so  $r_{AM}(t)$  can be written as

$$r_{AM}(t) = \sum_{l=1}^L A_l (1 + m x_l(t)) e^{j(2\pi f_{c,l}t + \theta_l)}, \quad (2)$$

where  $L$  is the number of AM interferers,  $m$  the modulation index,  $x_l(t)$  the voice signal of interferer  $l$ ,  $A_l$  its amplitude,  $f_{c,l}$  its central frequency, and  $\theta_l$  its phase. A typical value of the modulation index for voice communication is  $m = 0.85$ . The noise signal  $w(t)$  is assumed to be AWGN.

In the multicarrier system, the data is transmitted over  $N_{MC}$  subcarriers at a rate of  $1/T$ . The time-domain signal of the multicarrier system consists of the sum of contributions of the  $N_{MC}$  carriers. If the transmitted data symbols have zero mean, and the number of carriers  $N_{MC}$  is sufficiently large ( $N_{MC} \geq 64$ ), the time domain samples of the MC signal can, according to the central limit theorem, be modelled as zero mean Gaussian distributed. Because in the B-VHF system the number of carriers equals 512 and zero mean data symbols are transmitted, both conditions are fulfilled and, as the scope of this contribution is the estimation of the AM interference signals, the considered situation can be simplified by modelling the multicarrier signal  $r_{MC}(t)$  as an extra Gaussian distributed term. The received signal  $r(t)$  can be rewritten as

$$r(t) = r_{AM}(t) + \tilde{w}(t), \quad (3)$$

where  $\tilde{w}(t)$  is the equivalent noise consisting of the AWGN  $w(t)$  and the multicarrier signal  $r_{MC}(t)$ . The variance of this equivalent (possibly colored) noise is denoted as  $\sigma^2$  and is mainly determined by the MC power.

## 3. ESTIMATION OF THE AM INTERFERERS

In the MC system, the received signal is sampled at a rate  $1/T$ . To keep the overhead for the AM interference estimator as small as possible, we want to estimate the AM signal samples  $r_{AM}(kT)$  using the available samples  $r(kT)$ . The AM signal samples can be rewritten as

$$r_{AM}(kT) = \sum_{l=1}^L \tilde{A}_l(kT) e^{j2\pi f_{c,l}kT} \quad (4)$$

with  $\tilde{A}_l(kT)$  defined as

$$\tilde{A}_l(kT) = A_l (1 + m x_l(kT)) e^{j\theta_l}. \quad (5)$$

The equivalent amplitudes  $\tilde{A}_l(kT)$  are slowly varying functions of the time index  $k$  because the bandwidth of the AM signal is small as compared to the bandwidth  $1/T$  of the multicarrier system. Hence, it follows from (4) that the parameters to be estimated are the number of interferers  $L$ , the central frequencies  $\{f_{c,l}\}$ , and the time-varying amplitudes  $\{\tilde{A}_l(kT)\}$ ,  $l = 1, \dots, L$ .

To estimate the number of interferers  $L$  and the central frequencies  $\{f_{c,l}\}$  of the interferers, an ad hoc algorithm is considered. First, an  $N$ -point discrete Fourier transform (DFT) is applied to a block of  $N$  samples of the received signal  $\{r(kT) \mid k = 0, \dots, N-1\}$ . This DFT can easily be implemented as a fast Fourier transform (FFT). This results in

$$y(n) = \frac{1}{\sqrt{N}} \sum_{k=0}^{N-1} r(kT) e^{-j2\pi(kn/N)} = y_{AM}(n) + W(n), \quad (6)$$

where

$$y_{AM}(n) = \frac{1}{\sqrt{N}} \sum_{k=0}^{N-1} r_{AM}(kT) e^{-j2\pi(kn/N)} \quad (7)$$

and  $W(n)$  is the noise component with zero mean and variance  $\sigma^2$ .

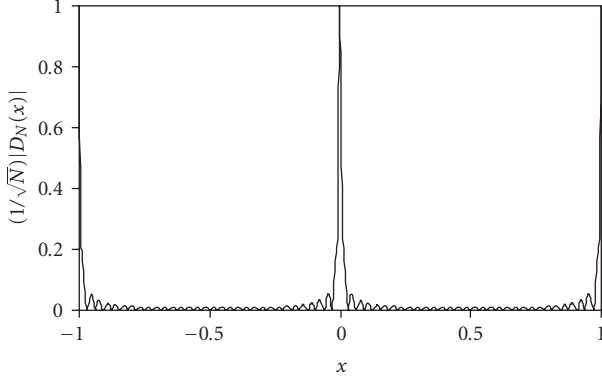
We assume that the equivalent amplitudes  $\{\tilde{A}_l(kT)\}$  are approximately constant for  $k = 0, \dots, N-1$ . This implies that, with respect to the determination of  $L$  and  $\{f_{c,l}\}$ , we approximate each narrowband AM interferer as a sinusoid with frequency  $f_{c,l}$  and amplitude  $\tilde{A}_l(0)$ . The DFT output corresponding to the AM signal is then given by

$$\begin{aligned} y_{AM}(n) &\approx \frac{1}{\sqrt{N}} \sum_{k=0}^{N-1} \sum_{l=1}^L \tilde{A}_l(0) e^{j2\pi f_{c,l}kT} e^{-j2\pi(kn/N)} \\ &= \sum_{l=1}^L \tilde{A}_l(0) D_N\left(\frac{n}{N} - f_{c,l}T\right), \end{aligned} \quad (8)$$

where

$$D_N(x) = \frac{1}{\sqrt{N}} \sum_{k=0}^{N-1} e^{-j2\pi kx} = \frac{1}{\sqrt{N}} e^{-j\pi(N-1)x} \frac{\sin(\pi Nx)}{\sin(\pi x)}. \quad (9)$$

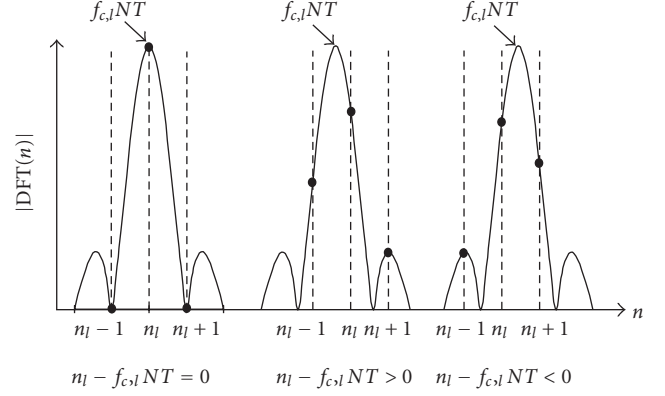
Figure 1 shows the function  $(1/\sqrt{N})|D_N(x)|$ . Note that this function is periodic and shows a peak with maximum 1 for

FIGURE 1: The function  $(1/\sqrt{N})|D_N(x)|$ , with  $N = 128$ .

integer values of  $x$ , while for noninteger values, the amplitude sharply drops. For increasing  $N$ , the width of the peak decreases while the value of  $(1/\sqrt{N})|D_N(x)|$  for noninteger values of  $x$  decreases. We assume that the interferers are spectrally separated, that is, the peaks for the interferers do not spectrally overlap. In most practical situations, this assumption is fulfilled. For example, an analog voice signal has typically a bandwidth of about 8 kHz. In the aeronautical communication system, the spectral separation between two AM modulated voice signals is at least 25 kHz to avoid interference between the AM signals. This assumption implies that for  $n \approx f_{c,l}NT$ , the sum in (8) reduces to one term. Therefore, the DFT output corresponding to the AM signal will show peaks at the indices  $n_l$  for which  $|f_{c,l} - n_l/NT| \approx 0$ ,  $l = 1, \dots, L$ .

The number of interferers  $L$  is determined by observing the amplitude of the output of the DFT and by counting the maxima. However, the presence of noise causes some peaks to be invisible (when the power of the AM interferer is small) or can introduce unwanted peaks. The inability to detect low-power AM signals will have only a small influence on the performance of the MC system, as such weak interferers only slightly disturb the multicarrier signal. On the other hand, estimation and elimination of an unwanted peak must be avoided because this will distort the multicarrier signal. To avoid this distortion, a threshold is introduced so that only peaks larger than this threshold will be selected for estimation and elimination. The threshold is selected such that the probability of an unwanted peak is smaller than a predetermined value that depends on the power of the multicarrier signal. If we assume that the unwanted peak is caused by the noise term  $W(n)$  only (no AM contribution is present), then the probability that the amplitude of the noise contribution is larger than the threshold  $\alpha$  is given by  $\Pr(\text{amplitude noise} > \alpha) = \exp(-\alpha^2/\sigma^2)$ .

The above-mentioned method results in  $\hat{L}$  detected peaks larger than the threshold. The index  $n_l$  corresponding to the  $l$ th detected peak yields a coarse estimate for the frequency of the  $l$ th AM signal,  $l = 1, \dots, \hat{L}$ . This estimate can be improved by observing (8) and Figure 2 which shows the influence of  $f_{c,l}$  on the output of the DFT. For values of  $n$  close to  $n_l$ , (8)

FIGURE 2: Influence of  $f_{c,l}$  on the output of the DFT.

reduces to  $\tilde{A}_l(0)D_N(n/N - f_{c,l}T)$  because the contributions of the other terms can be neglected. We can determine the shift  $\epsilon_l = n_l/N - f_{c,l}T$  by observing  $y_{AM}(n_l \pm 1)$ . The effect of  $\tilde{A}_l(0)$  can be eliminated by computing the ratios  $y_{AM}(n_l)/y_{AM}(n_l \pm 1)$ . Taking into account the definition of  $D_N(x)$  (9), these ratios can be approximated by

$$\frac{y_{AM}(n_l)}{y_{AM}(n_l + 1)} = e^{-j(\pi/N)} \frac{\sin(\pi(\epsilon_l + 1/N))}{\sin(\pi\epsilon_l)} \approx e^{-j(\pi/N)} \left(1 + \frac{1}{N\epsilon_l}\right), \quad (10)$$

$$\frac{y_{AM}(n_l)}{y_{AM}(n_l - 1)} = e^{+j(\pi/N)} \frac{\sin(\pi(\epsilon_l - 1/N))}{\sin(\pi\epsilon_l)} \approx e^{+j(\pi/N)} \left(1 - \frac{1}{N\epsilon_l}\right), \quad (11)$$

where we assumed that  $\epsilon_l$  is small. At the receiver side, the samples  $y_{AM}(n)$  are not available, so we define  $\Delta_{\pm 1} = y(n_l)/y(n_l \pm 1)$ . The samples  $y(n)$  contain a noise component, such that the estimation of  $\epsilon_l$  is affected by the noise. The effect of the noise on the estimate will be smaller when the amplitude of  $y_{AM}(n_l \pm 1)$  is larger, so we only use the largest of the two DFT outputs  $|y(n_l \pm 1)|$  for estimating  $\epsilon_l$ . The estimate of the shift  $\hat{\epsilon}_l$  can then be approximated by

$$\hat{\epsilon}_l \approx \begin{cases} \frac{1}{N(\Re(\Delta_{+1}e^{+j(\pi/N)}) - 1)} & \text{if } |\Delta_{+1}| < |\Delta_{-1}|, \\ \frac{-1}{N(\Re(\Delta_{-1}e^{-j(\pi/N)}) - 1)} & \text{if } |\Delta_{+1}| > |\Delta_{-1}|. \end{cases} \quad (12)$$

However, if  $n_l \approx f_{c,l}NT$ , the estimated  $\hat{\epsilon}_l$  will be unreliable and can be larger than  $1/(2N)$  because in that case  $y_{AM}(n_l \pm 1)$  is close to zero, as can be seen from Figure 2, such that  $y(n_l \pm 1)$  contains mainly noise. However, in this case, the

coarse estimate is an accurate estimate, so when  $|\hat{\epsilon}_l| > 1/(2N)$ , no correction is applied and the frequency estimate is given by

$$\hat{f}_{c,l} = \frac{n_l}{NT}. \quad (13)$$

By increasing  $N$ , the coarse estimate can become more accurate, as the difference  $|\hat{f}_{c,l} - n_l/NT| < 1/NT$  decreases with increasing  $N$ . However, we made the assumption that  $\tilde{A}_l(kT)$  is approximately constant over the  $N$  samples. When we increase  $N$ , this assumption will not hold, such that the fine estimates from (12) will become less reliable.

In this first step, we have determined the number of interferers  $\hat{L}$ , and for each AM interferer, an estimate of the central frequency  $\hat{f}_{c,l}$  has been obtained,  $l = 1, \dots, \hat{L}$ . In the second step, we estimate the amplitude of the  $l$ th AM signal with the following estimator:

$$\hat{A}_l(nT) = \frac{1}{2K+1} \sum_{k=-K}^K r((n+k)T) e^{-j2\pi(n+k)\hat{f}_{c,l}T}. \quad (14)$$

First, the  $l$ th AM signal is downconverted to its baseband by multiplying the received signal samples with  $\exp(-j2\pi k\hat{f}_{c,l}T)$ . The estimate of the amplitude of the  $l$ th AM signal is obtained by averaging the resulting samples over a  $(2K+1)$  size sliding window. This averaging acts as a lowpass filter with bandwidth  $1/(2K+1)T$ , which reduces the effects of the noise and the contributions of the other AM signals with frequencies  $\hat{f}_{c,l'} - \hat{f}_{c,l}$ , so containing mainly high-frequency components with respect to the window size. The effects of noise and disturbing AM signals can be further reduced by increasing  $K$ , which results in reducing the bandwidth of the equivalent lowpass filter; but if the bandwidth of the equivalent lowpass filter becomes smaller than the bandwidth of the AM signals, which means that  $K$  is selected too large, the sliding window will not be able to track the fast variations of the wanted AM signals. Hence, an optimal value of the window size can be found. Note that a small estimation error of the central frequency  $\hat{f}_{c,l}$  will result in a slow-time variation of the amplitude, which can easily be tracked by the amplitude estimator (14). Hence, the proposed algorithm is robust to small estimation errors of the central frequency.

#### 4. PERFORMANCE EVALUATION

In this section, we derive the mean square error (MSE) for the amplitude, assuming perfect frequency estimation. This assumption is valid because it will be shown in the numerical results that the MSE for the frequency estimation is very low. We assume that  $A_l$  is real-valued and the real-valued voice signal  $x_l(t)$  has zero mean,  $l = 1, \dots, L$ . We define  $R_l(t)$  as the autocorrelation function and  $S_l(f)$  as the spectrum of  $x_l(t)$ :

$$\begin{aligned} R_l(t) &= E[x_l(\tau)x_l(t+\tau)], \\ S_l(f) &= \text{FT}(R_l(t)), \end{aligned} \quad (15)$$

where  $\text{FT}(\cdot)$  denotes the Fourier transform. The MSE of the amplitude can be written as (see the appendix for the computation)

$$\begin{aligned} \sigma_{\tilde{A}_l}^2 &= A_l^2 m^2 \int_{-\infty}^{+\infty} S_l(f) (F_K(fT) - 1)^2 df \\ &+ \sum_{l'=1; l' \neq l}^L A_{l'}^2 \left( (F_K(\Delta f_{l',l}T))^2 \right. \\ &\quad \left. + m^2 \int_{-\infty}^{+\infty} S_{l'}(f) (F_K((f + \Delta f_{l',l})T))^2 df \right) \\ &+ \frac{\sigma^2}{2K+1}, \end{aligned} \quad (16)$$

where  $\Delta f_{l',l} = f_{c,l'} - f_{c,l}$  and

$$F_K(x) = \frac{1}{2K+1} \sum_{k=-K}^K e^{j2\pi kx} = \frac{1}{2K+1} \frac{\sin(\pi(2K+1)x)}{\sin(\pi x)}. \quad (17)$$

When the amplitude  $\tilde{A}_l(nT)$  can be considered as constant over the interval  $[(n-K)T, (n+K)T]$ ,  $l = 1, \dots, L$ , that is, for sufficiently small  $K$ , the MSE (16) reduces to

$$\sigma_{\tilde{A}_l}^2 = \frac{\sigma^2}{2K+1} + \sum_{l'=1; l' \neq l}^L P_{l'} (F_K(\Delta f_{l',l}T))^2, \quad (18)$$

where we defined  $P_l = A_l^2 (1 + m^2 R_l(0))$  as the power of the  $l$ th AM signal.

#### 5. SUCCESSIVE INTERFERENCE CANCELLATION

The second term in (16) implies that the estimation of the amplitude of an AM interference signal is disturbed by the presence of other AM signals. This disturbance increases with increasing number of AM signals. Further, weak AM signals will suffer more from the disturbance of other AM signals (especially when the other AM signals are stronger) than strong AM signals. Therefore, we propose to improve the performance of the previous estimator by successively estimating and cancelling the AM signals. Based on the DFT outputs of the frequency estimator, we rank the detected AM signals from strong to weak.

First, an estimate of the amplitude of the strongest AM interferer is obtained with the previously described sliding window method. Then, this AM interferer is removed by subtracting the estimated AM signal from the received signal samples  $r(kT)$ . Next, the amplitude of the second strongest AM interferer is estimated with the sliding window method. Hence, to estimate the amplitude of the  $l$ th AM signal, the  $l-1$  stronger AM signals are canceled from the received signal and based on the resulting signal, an estimate of the amplitude of the  $l$ th AM signal is made using the sliding window method. Successive interference cancellation results in better estimates of the amplitudes of the AM interferers at the cost

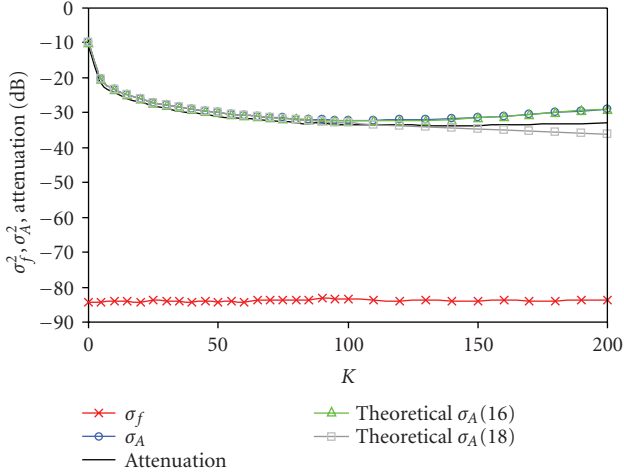


FIGURE 3: MSE and attenuation for one AM interferer ( $L = 1$ ),  $A_I = 1$ ,  $N f_{c,l} T = 10.76$ ,  $m = 0.85$ ,  $\sigma^2 = -10$  dB.

of a higher complexity: to estimate  $N$  values of the amplitude of the weakest AM interferer,  $N + 2K$  successive modified received signal samples are needed, which means that also an estimate of the amplitude of the other  $L - 1$  AM interferers for these  $N + 2K$  samples is needed. To estimate the amplitude of the second weakest AM interferer, we need the estimate of the previous  $L - 2$  AM interferers in  $N + 4K$  successive samples. The algorithm requires the estimate of the amplitude of the strongest AM interferer in  $N + (L - 1)2K$  successive samples, and to estimate the amplitude of the strongest AM interferer, we need  $N + 2LK$  successive samples of the received signal.

### 6. NUMERICAL RESULTS

For the simulations, we consider an MC system with a sampling rate of  $1/T = 1/0.9375 \mu\text{s}$  and an FFT with length  $N = 512$ . The voice signals  $x_l(t)$  are generated with the B-VHF voice signal generator [8]. The sum of the MC signals and noise is generated as AWGN.

Figure 3 shows the MSE of the frequency estimate and the amplitude estimate for the case of one AM interferer ( $L = 1$ ) with amplitude  $A_I = 1$  and the noise level equals  $\sigma^2 = -10$  dB. The frequency estimator is very accurate as the MSE of the frequency estimate is very low. The theoretical expressions for the MSE of the amplitude (16) and (18) are compared with the numerical results from the simulations. We can see that the simulation results agree well with the theoretical result (16) for all values of  $K$ . However, to compute (16), the spectra of the AM signals  $S_l(f)$  must be known which are not always available. If only the powers  $P_l$  of the AM signals are available, expression (18) can be used. This expression shows a good accordance with the simulation results for sufficiently small window size  $K$ , where the assumption that the time-varying amplitude  $\tilde{A}_l(nT)$  is constant over the window is valid. Figure 3 also shows the attenuation, which is defined as the difference between the power of the AM signal after and before elimination. We notice that

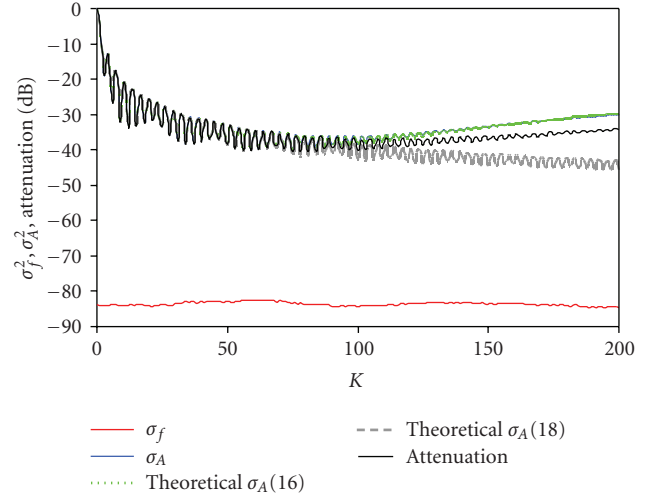


FIGURE 4: MSE and attenuation for two AM interferers ( $L = 2$ ),  $A_I = [1 \ 1]$ ,  $N f_{c,l} T = [10.76 \ 92.36]$ ,  $m = 0.85$ ,  $\sigma^2 = -20$  dB.

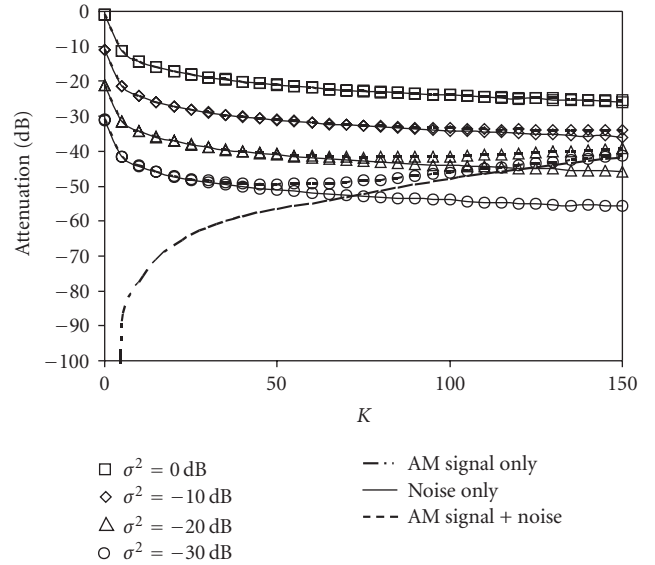


FIGURE 5: MSE and attenuation for one AM interferer ( $L = 1$ ),  $A_I = 1$ ,  $N f_{c,l} T = 10.76$ ,  $m = 0.85$ ,  $\sigma^2 = -10$  dB.

the attenuation almost coincides with the MSE of the estimate of the amplitude which indicates that the estimation errors of the frequencies can be neglected.

In Figure 4, the MSE of the frequency and amplitude estimates are shown together with the attenuation for the case of two AM interferers ( $L = 2$ ). We can draw similar conclusions as in Figure 3. The second AM signal affects the estimation error: the MSE of the amplitude shows an oscillation. This is caused by the second term in (16) and (18) because the function  $F_K(\Delta f_{l,l} T)$  is a periodic function with frequency  $\Delta f_{l,l}$ .

Figure 5 shows the simulation results for the attenuation of the AM signal obtained with the proposed estimator for  $L = 1$  (note that both methods for estimating the amplitude of the AM interferer are the same if there is only one

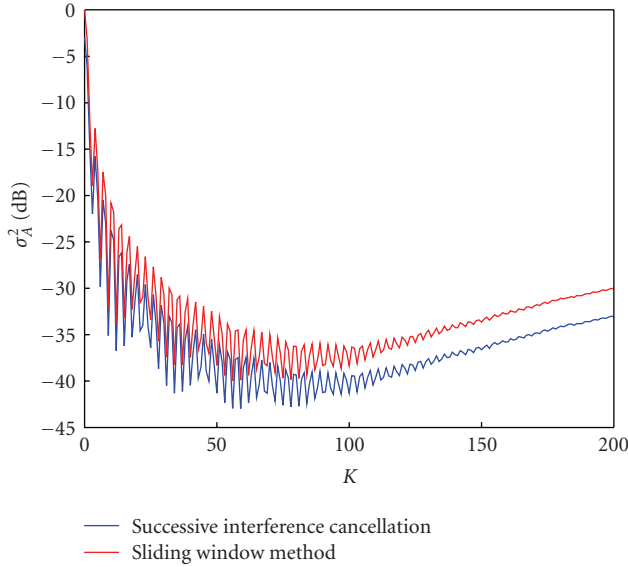


FIGURE 6: MSE for two AM interferers ( $L = 2$ ),  $A_I = [1 \ 1]$ ,  $Nf_{c,i}T = [10.76 \ 92.36]$ ,  $m = 0.85$ ,  $\sigma^2 = -20$  dB.

AM interferer to estimate) for different values of the MC signal plus noise level  $\sigma^2$ . Theoretical results are also shown for the cases of AM signal only (no noise present), corresponding to the first term in (16), and noise only (no AM signal present), corresponding to the last term in (16). The attenuation is dominated by the noise for small values of  $K$  because the time variation of the amplitude can be neglected. By increasing  $K$ , the noise is better averaged out. The time variation of the amplitude becomes important for large values of  $K$  because the estimator cannot track the fast variations of the amplitude as the window size is too large: the AM signal is approximated by the estimator as a sinusoid with constant amplitude. The optimum value of  $K$  depends on the bandwidth of the AM signal and the noise level. We observe that when the noise level decreases, the optimum value of  $K$  also decreases because the noise averaging becomes less important than the time variation of the AM signal. Note that the optimum value of the attenuation is approximately 20 dB lower than the noise level  $\sigma^2$ : the estimator is able to reduce the AM signal power to roughly 20 dB below the power of the MC signal.

In Figure 6, the two estimators for the amplitude of the AM signals are compared in terms of the MSE of the amplitude estimate for the same situation as in Figure 4. The simulation results indicate that successive interference cancellation gives rise to an MSE that is 3 dB below the MSE for the sliding window method in this case.

Figure 7 shows the influence of the threshold on the attenuation for the case of one AM interferer ( $L = 1$ ) for different values of  $\sigma^2$ . At low values of the threshold, the probability of a false detect increases, as more unwanted peaks are detected. This causes a distortion of the MC signal, resulting in performance degradation. At high values of the threshold, the probability of a false miss, that is, the inability to detect

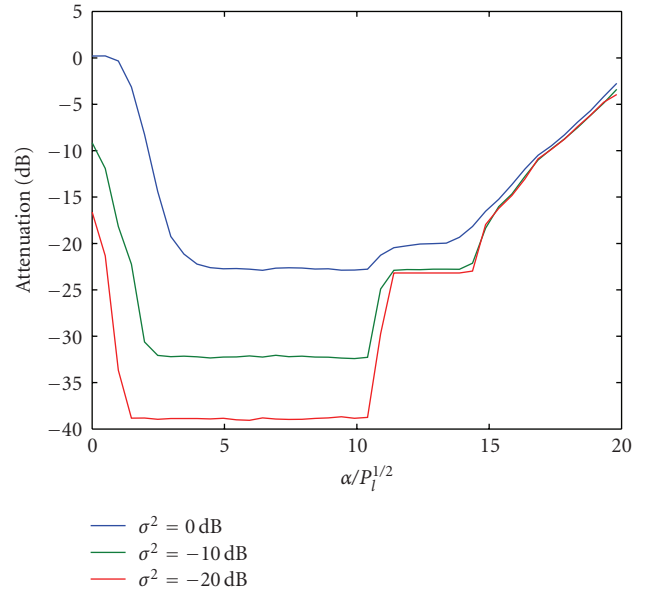


FIGURE 7: Attenuation for one AM interferer ( $L = 1$ ),  $A_I = 1$ ,  $Nf_{c,i}T = 10.76$ ,  $m = 0.85$ .

a peak, increases. When no AM signal is detected, it can also not be eliminated, resulting in a reduction of the average attenuation that can be obtained. We can see that a good choice of the threshold minimizes the attenuation independently of  $\sigma^2$ .

Now we consider an OFDM system with 512 carriers in two cases. In both cases, we consider a frequency gap of  $M$  carriers to cope with a possible interferer within the B-VHF cell, so only  $N - M$  carriers are filled with data symbols. This means that the average transmitted power per sample is reduced to  $P_{\text{OFDM}} = ((N - M)/N)E_s$ . The power of the AM interferer is approximately given by  $P_{\text{AM}} \approx A^2$ , so the signal-to-interference ratio (SIR) is defined as  $((N - M)/N)(E_s/A^2)$ . In both cases, we assume one interferer is present. In the first case, the AM interferer is located within the B-VHF cell, and the  $M$  unused carriers of the B-VHF system are centered around this interferer. In Figure 8, the BER is shown for the OFDM system with and without interference cancellation for an  $\text{SIR} \approx -20$  dB (dashed lines). The BER for BPSK modulation is also shown which serves as a lower bound for the BER of the considered OFDM system. The performance of the OFDM system with interference cancellation is close to optimum for a wide range of  $E_s/N_0$  and has a gain of 5 dB compared to the OFDM system without interference cancellation. For the higher  $E_s/N_0$ , there exists an error floor as the proposed algorithm cannot eliminate the fast changes of the AM interferer. In the second case, also shown in Figure 8 (solid lines), all interferers within the B-VHF cell are inactive, and only one AM interferer from a neighboring cell is present, having an  $\text{SIR} \approx -20$  dB. This interferer is located outside the frequency gap of  $M$  carriers. The performance of the OFDM system is reduced, but performing interference cancellation still gives (in this figure) a gain of 3 dB compared to an OFDM system without interference cancellation. The

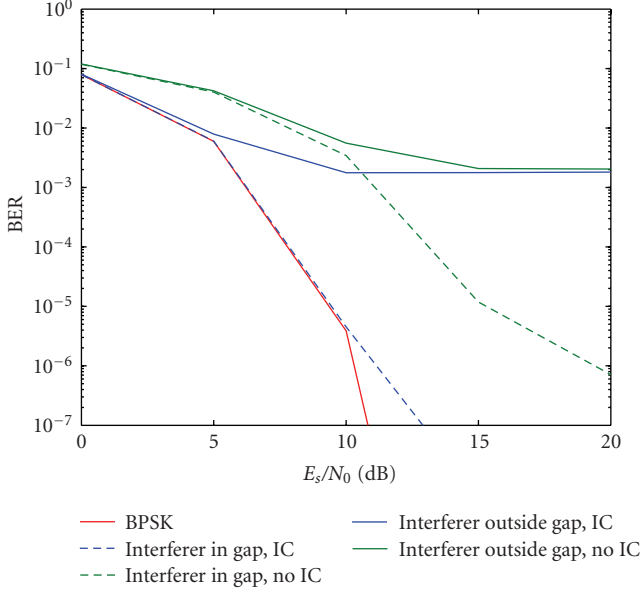


FIGURE 8: BER for an OFDM system ( $E_s = 1$ ,  $N = 512$ ,  $M = 12$ ) in the presence of 1 interferer ( $A = \sqrt{100}$ ).

error floor is close to  $10^{-3}$  which is the target BER for voice communication. This error floor is caused by the fact that the data symbols transmitted on the carriers close to the central frequency of the AM interferer are destroyed. In our case ( $SIR \approx -20$  dB), the side lobes of the AM interferer (after cancellation) are weaker than the OFDM signal, but the central frequency is strong enough to disturb the OFDM signal. This results in the 2 carriers closest to the central frequency of the AM interferer to be lost, so the BER floor is approximately given by  $2/(512 - 12) \times 1/2 = 2 \cdot 10^{-3}$ . Decreasing the SIR will cause the sidelobes of the AM interferer to become more important which results in a higher BER floor as more carriers will possibly be destroyed.

## 7. CONCLUSION

In this paper, we have proposed two AM signal estimators, that is, the sliding window estimator and the successive interference cancellation algorithm, to reduce the effect of the AM interference in an overlay multicarrier system. Both estimators use the same frequency estimation method but differ in the way in which the time-varying amplitudes of the AM signals are estimated. For the sliding window estimator, we have derived the MSE of the amplitude estimate in an analytical way. Simulation results confirm the theoretical expressions. Simulations also indicate that the attenuation is independent of frequency estimation errors, but is mainly determined by the amplitude estimation errors. An attenuation of the AM signal of approximately 20 dB below the multicarrier signal power can be obtained. For more than one AM interferer, the successive interference cancellation algorithm outperforms the sliding window estimator in terms of attenuation. Further, the numerical results show that the OFDM system with interference cancellation has a considerably lower BER com-

pared to an OFDM system without interference cancellation. If we would combine the proposed algorithm with the time domain windowing from [10], this would result in an extra performance improvement: the BER of the OFDM system will slightly decrease.

## APPENDIX

### A COMPUTATION OF $\sigma_{\hat{A}_I}^2$

Starting from (14) and using (3) and (4), the estimate  $\hat{\tilde{A}}_I(nT)$  can be rewritten as

$$\begin{aligned} \hat{\tilde{A}}_I(nT) &= \frac{1}{2K+1} \sum_{l'=1}^L \sum_{k=-K}^K \tilde{A}_{l'}((n+k)T) e^{j2\pi(n+k)(f_{c,l'} - f_{c,l})T} \\ &\quad + \frac{1}{2K+1} \sum_{k=-K}^K \tilde{w}((n+k)T), \end{aligned} \quad (\text{A.1})$$

and the MSE of the estimate of  $\tilde{A}_I(nT)$  is defined as

$$\sigma_{\hat{A}_I}^2 = E \left[ \left| \hat{\tilde{A}}_I(nT) - \tilde{A}_I(nT) \right|^2 \right]. \quad (\text{A.2})$$

This MSE can be written as a sum of three components:

$$\begin{aligned} \sigma_{\hat{A}_I}^2 &= E \left[ \left| \frac{1}{2K+1} \sum_{k=-K}^K (\tilde{A}_I((n+k)T) - \tilde{A}_I(nT)) \right|^2 \right] \\ &\quad + E \left[ \left| \frac{1}{2K+1} \sum_{l'=1, l' \neq l}^L \sum_{k=-K}^K \tilde{A}_{l'}((n+k)T) e^{j2\pi(n+k)(f_{c,l'} - f_{c,l})T} \right|^2 \right] \\ &\quad + E \left[ \left| \frac{1}{2K+1} \sum_{k=-K}^K \tilde{w}((n+k)T) \right|^2 \right]. \end{aligned} \quad (\text{A.3})$$

The first component can be rewritten as

$$\begin{aligned} &E \left[ \left| \frac{1}{2K+1} \sum_{k=-K}^K (\tilde{A}_I((n+k)T) - \tilde{A}_I(nT)) \right|^2 \right] \\ &= \frac{1}{(2K+1)^2} \sum_{k=-K}^K \sum_{k'=-K}^K A_I^2 m^2 (R_I(k-k') - 2R_I(k) + R_I(0)), \end{aligned} \quad (\text{A.4})$$

where we used the definition of  $\tilde{A}_I(nT)$  (5) and the definition of  $R_I(k)$  (15). Using the relationship between  $R_I(k)$  and  $S_I(k)$ , this result can be rewritten as

$$\begin{aligned} &E \left[ \left| \frac{1}{2K+1} \sum_{k=-K}^K (\tilde{A}_I((n+k)T) - \tilde{A}_I(nT)) \right|^2 \right] \\ &= A_I^2 m^2 \int_{-\infty}^{+\infty} S_I(f) (F_K(fT) - 1)^2 df, \end{aligned} \quad (\text{A.5})$$

where  $F_K(x)$  is defined in (17).

The second term of (A.3) can be written as

$$\begin{aligned}
 & E \left[ \left| \frac{1}{2K+1} \sum_{l'=1; l' \neq l}^L \sum_{k=-K}^K \tilde{A}_{l'}((n+k)T) e^{j2\pi(n+k)(f_{c,l'} - f_{c,l})T} \right|^2 \right] \\
 &= \frac{1}{(2K+1)^2} \sum_{l'=1; l' \neq l}^L \sum_{k=-K}^K \\
 &\quad \times \sum_{k'=-K}^K A_{l'}^2 (1+m^2 R_l(k-k')) e^{j2\pi(k-k')(f_{c,l'} - f_{c,l})T}.
 \end{aligned} \tag{A.6}$$

Exploiting (15) and (17) yields that

$$\begin{aligned}
 & E \left[ \left| \frac{1}{2K+1} \sum_{l'=1; l' \neq l}^L \sum_{k=-K}^K \tilde{A}_{l'}((n+k)T) e^{j2\pi(n+k)(f_{c,l'} - f_{c,l})T} \right|^2 \right] \\
 &= \sum_{l'=1; l' \neq l}^L A_{l'}^2 (F_K(\Delta f_{l',l}))^2 + A_{l'}^2 m^2 \int_{-\infty}^{+\infty} S_{l'}(f) (F_K(\Delta f_{l',l}))^2 df.
 \end{aligned} \tag{A.7}$$

The third component of (A.3) is the noise term and can easily be found to be

$$E \left[ \left| \frac{1}{2K+1} \sum_{k=-K}^K \tilde{w}((n+k)T) \right|^2 \right] = \frac{\sigma^2}{2K+1}. \tag{A.8}$$

Collecting the results of (A.5), (A.7), and (A.8) yields (16).

## REFERENCES

- [1] J. A. C. Bingham, "Multicarrier modulation for data transmission: an idea whose time has come," *IEEE Communications Magazine*, vol. 28, no. 5, pp. 5–14, 1990.
- [2] K. Maxwell, "Asymmetric digital subscriber line: interim technology for the next forty years," *IEEE Communications Magazine*, vol. 34, no. 10, pp. 100–106, 1996.
- [3] European Telecommunications Standards Institute, "Broadband radio access networks (BRAN); HIPERLAN Type 2; Physical (PHY) layer," France, TR 101 475 V.1.1.1, April 2000.
- [4] IEEE 802.11, "Wireless LAN Medium Access Control (MAC) Physical Layer (PHY) Specifications, Amendment 1: High-Speed Physical Layer in the 5 GHz Band," July 1999.
- [5] European Telecommunications Standards Institute, "Digital audio broadcasting (DAB); DAB to mobile portable and fixed receivers," France, ETS 300 401, February 1995.
- [6] European Telecommunications Standards Institute, "Digital video broadcasting (DVB); Framing structure, channel coding and modulation for 11/12 GHz satellite services," France, ETS 300 421, December 1994.
- [7] M. Schnell, E. Haas, M. Sajatovic, C. Rihacek, and B. Haindl, "B-VHF—an overlay system concept for future ATC communications in the VHF band," in *Proceedings of the 23rd Digital Avionics Systems Conference (DASC '04)*, vol. 1, pp. 1–2, Salt Lake City, Utah, USA, October 2004.
- [8] <http://www.b-vhf.org/>.
- [9] S. Brandes, M. Schnell, and C.-H. Rokitansky, "B-VHF—selected simulation results and assessment," in *Proceedings of the 25th Digital Avionics Systems Conference (DASC '06)*, pp. 1–12, Portland, Ore, USA, October 2006.
- [10] S. Brandes, I. Cosovic, and M. Schnell, "Techniques for ensuring co-existence between BVHF and legacy VHF systems," in *Proceedings of the IEEE Aerospace Conference*, Washington, DC, USA, October 2006.
- [11] D. Van Weiden and H. Steendam, "Interference cancellation of AM narrowband interference signals," in *Proceedings of the 65th IEEE Vehicular Technology Conference (VTC '07)*, pp. 1617–1621, Dublin, Ireland, April 2007.

## Special Issue on Human-Centric Applications of Distributed Camera Networks

### Call for Papers

In a camera network, access to multiple sources of visual data often allows for making more comprehensive interpretation of events and activities. Vision-based sensing fits well within the notion of pervasive sensing and computing environments, enabling novel user-centric applications. In such applications, the actions of the users and their interactions with the environment are detected and interpreted by the network of cameras, and proper services or responses are offered based on the context.

Gesture recognition problems have been extensively studied in human computer interactions (HCIs), where often a set of predefined gestures is used for delivering instructions to machines. However, passive gestures predominate in behavior descriptions in many applications. Some traditional application examples include surveillance and security applications, while novel application classes arise in emergency detection in elderly care and assisted living, video conferencing, creating human models for gaming and virtual environments, and biomechanics applications analyzing human movements. Through pervasive visual sensing and collaborative processing, distributed camera networks offer the potential of a generalized HCI environment, in which the network reacts to various intentional gestures of the users stated, for example, via hand movements or gazing at a region of interest, as well as to unintentional posture changes caused by events such as accidental falls in assisted living applications.

Application development based on visual information obtained via multiple cameras requires new methodologies to efficiently fuse the data in the network. In a multi camera network, the option to employ local processing of acquired video at the source camera facilitates operation of scalable vision networks by avoiding transfer of raw images. Embedded processing utilizes the increasingly available computing power at the source to extract features from the images, which are exchanged with other cameras. Additional motivation for distributed processing stems from an effort to preserve privacy of the network users while offering services in applications such as assisted living. In a distributed processing framework, data fusion can occur across the three dimensions of 3D space (multiple views), time, and feature levels.

The goal of this special issue is to provide a coverage of the various approaches to human-centric application development in a multi camera setting. In particular, approaches based on the distributed processing of acquired video sequences, model-based approaches for human behavior monitoring, vision-based information fusion and collaborative decision making, and interfaces between the vision network and high-level reasoning modules that provide interpretative deductions will fit well within the scope of the special issue. The special issue also aims to provide insight into algorithm and system development topics pertaining to real-world application design for smart environments.

Original papers, previously unpublished and not currently under review by another journal, are solicited to cover one or more of the following topics:

- Distributed and collaborative vision algorithms for human-centric applications
- Model-based human gesture recognition in camera networks
- Motion analysis and spatial reasoning for behavior models
- Spatiotemporal data and estimate fusion techniques
- High-level interpretation of human activities
- Activity monitoring in crowds
- Environment discovery
- Detection of abnormal behavior
- Applications in smart homes and other environments

Authors should follow the EURASIP Journal on Image and Video Processing manuscript format described at the journal site <http://www.hindawi.com/journals/ivp/>. Prospective authors should submit an electronic copy of their complete manuscripts through the journal Manuscript Tracking System at <http://mts.hindawi.com/>, according to the following timetable:

Manuscript Due	March 1, 2008
First Round of Reviews	June 1, 2008
Publication Date	September 1, 2008

# EURASIP Journal on Image and Video Processing

## Guest Editors

**Hamid Aghajan**, Stanford University, CA, USA;  
hamid@wsnl.stanford.edu

**Richard Kleihorst**, NXP Semiconductors Research,  
Eindhoven, The Netherlands; richard.kleihorst@nxp.com

**Bernhard Rinner**, University of Klagenfurt, Carinthia,  
Austria; bernhard.rinner@uni-klu.ac.at

**Wayne Wolf**, Georgia Institute of Technology, GA, USA;  
wolf@ece.gatech.edu

## Special Issue on Active Antennas for Space Applications

### Call for Papers

Over the last years, many journal articles appeared on the principles, analysis, and design of active and active integrated antennas (AAs and AIAs). An AA is a single system comprising both a radiating element and one or more active components which are tightly integrated. This gives clear advantages in terms of costs, dimensions, and efficiency. In the case of an AIA, both the active device and the radiator are integrated on the same substrate. Both options lead to very compact, low-loss, flexible antennas, and this is very important especially at high frequencies, such as those typical of a satellite link. As microwave integrated-circuit and the microwave monolithic integrated-circuit technologies have ripened, AA and AIA applications have become more and more interesting, not only at a scientific level but also from a commercial point of view, up to the point that they have recently been applied to phased array antennas on board moving vehicles for satellite broadband communication systems.

The goal of this special issue is to present the most recent developments and researches in this field, with particular attention to space-borne applications, as well as to enhance the state of the art and show how AAs and AIAs can meet the challenge of the XXI century telecommunications applications.

Topics of interest include, but are not limited to:

- Active (integrated) antenna design, analysis, and simulation techniques
- Active (integrated) antenna applications in arrays, retrodirective arrays and discrete lenses
- Millimeter-wave active (integrated) antennas

Authors should follow International Journal of Antennas and Propagation manuscript format described at the journal site <http://www.hindawi.com/journals/ijap/>. Prospective authors should submit an electronic copy of their complete manuscript through the journal Manuscript Tracking System at <http://mts.hindawi.com/>, according to the following timetable:

Manuscript Due	September 1, 2008
First Round of Reviews	December 1, 2008
Publication Date	March 1, 2009

### Guest Editors

**Stefano Selleri**, Department of Electronics and Telecommunications, University of Florence, Via C. Lombroso 6/17, 50137 Florence, Italy; [stefano.selleri@unifi.it](mailto:stefano.selleri@unifi.it)

**Giovanni Toso**, European Space Research and Technology Center (ESTEC), European Space Agency (ESA), Keplerlaan 1, PB 299, 2200 AG Noordwijk, The Netherlands; [giovanni.toso@esa.int](mailto:giovanni.toso@esa.int)

## Special Issue on Secure Steganography in Multimedia Content

### Call for Papers

Steganography, the art and science of invisible communication, aims to transmit information that is embedded invisibly into carrier data. Different from cryptography it hides the very existence of the secret. Its main requirement is undetectability, that is, no method should be able to detect a hidden message in carrier data.

The theoretical foundations of steganography and detection theory have been advanced rapidly, resulting in improved steganographic algorithms as well as more accurate models of their capacity and weaknesses.

However, the field of steganography still faces many challenges. Recent research in steganography and steganalysis has far-reaching connections to machine learning, coding theory, and signal processing. There are powerful blind (or universal) detection methods, which are not fine-tuned to a particular embedding method, but detect steganographic changes using a classifier that is trained with features from known media. Coding theory facilitates increased embedding efficiency and adaptiveness to carrier data, both of which will increase the security of steganographic algorithms. Finally, both, practical secure steganographic algorithms and steganalytic methods require signal processing of common media like images, audio, and video.

This journal has a particular emphasis on the reproducibility of results and the comparison among competing schemes, and experimental evaluation, that is, papers whose goal is that of comparing existing systems, testing existing algorithms against new data sets, reporting experimental evidence that results published by someone else are incorrect or incorrectly interpreted (in this last case software sharing is a mandatory requirement).

The main goal of this special issue is to provide a state-of-the-art view on current research in the field of steganographic applications. Some of the related research topics for the submission include, but are not limited to:

- Information-theoretic aspects of secure steganography
- Performance, complexity, and security analysis of steganographic methods
- Practical secure steganographic methods for images, audio, video, and more exotic media and bounds on detection reliability

- Adaptive, content-aware embedding in various transform domains
- Large-scale experimental setups and carrier modeling
- Energy-efficient realization of embedding pertaining encoding and encryption
- Steganographic applications and protocols
- Interplay between capacity, embedding efficiency, coding and detectability
- Steganalytic application in steganography benchmarking and digital forensics
- Attacks against steganalytic applications

Authors should follow the EURASIP Journal on Information Security manuscript format described at the journal site <http://www.hindawi.com/journals/is/>. Prospective authors should submit an electronic copy of their complete manuscript through the journal Manuscript Tracking System at <http://mts.hindawi.com/> according to the following timetable:

Manuscript Due	August 1, 2008
First Round of Reviews	November 1, 2008
Publication Date	February 1, 2009

### Guest Editors

**Miroslav Goljan**, Department of Electrical and Computer Engineering, Watson School of Engineering and Applied Science, Binghamton University, P.O. Box 6000, Binghamton, NY 13902-6000, USA; [mgoljan@binghamton.edu](mailto:mgoljan@binghamton.edu)

**Andreas Westfeld**, Institute for System Architecture, Faculty of Computer Science, Dresden University of Technology, Helmholtzstraße 10, 01069 Dresden, Germany; [westfeld@inf.tu-dresden.de](mailto:westfeld@inf.tu-dresden.de)

## Special Issue on Wireless Access in Vehicular Environments

### Call for Papers

Wireless access in vehicular environments (WAVE) technology comes into sight as a state-of-the-art solution to contemporary vehicular communications, which is anticipated to be widely applied in the near future to radically improve the transportation environment in aspects of safety, intelligent management, and data exchange services. WAVE systems will fundamentally smooth the progress of intelligent transportation systems (ITSs) by providing them with high-performance physical platforms. WAVE systems will build upon the IEEE 802.11p standard, which is still active and expected to be ratified in April, 2009. Meanwhile, the VHF/UHF (700 MHz) band vehicular communication systems are attracting increasingly attention recently.

The fast varying and harsh vehicular environment brings about several fresh research topics on the study of WAVE systems and future vehicular communication systems, which include physical layer challenges associated with mobile channels, capacity evaluation, novel network configuration, effective media access control (MAC) protocols, and robust routing and congestion control schemes.

The objective of this special section is to gather and circulate recent progresses in this fast developing area of WAVE and future vehicular communication systems spanning from theoretical analysis to testbed setup, and from physical/MAC layers' enabling technology to network protocol. These research and implementation activities will be considerably helpful to the design of WAVE and future vehicular communications systems by removing major technical barriers and presenting theoretical guidance. This special issue will cover, but not limited to, the following main topics:

- 700 MHz/5.8 GHz vehicle-to-vehicle (V2V)/vehicle-to-infrastructure (V2I) single-input single-output (SISO)/MIMO channel measurement and modeling, channel spatial and temporal characteristics exploration
- Doppler shift study, evaluation and estimate, time and frequency synchronizations, channel estimate and prediction
- Utilization of MIMO, space-time coding, smart antenna, adaptive modulation and coding
- Performance study and capacity analysis of V2V and V2I communications operating over both 5.8GHz and 700Mz

- Software radio, cognitive radio, and dynamic spectrum access technologies applied to WAVE and future vehicular communication systems
- Mesh network and other novel network configurations for vehicular networks
- Efficient MAC protocols development
- Routing algorithms and congestion control schemes for both real-time traffic warning message broadcasting and high-speed data exchange
- Cross-layer design and optimization
- Testbed or prototype activities

Authors should follow the EURASIP Journal on Wireless Communications and Networking manuscript format described at the journal site <http://www.hindawi.com/journals/wcn/>. Prospective authors should submit an electronic copy of their complete manuscript through the EURASIP Journal on Wireless Communications and Networking's Manuscript Tracking System at <http://mts.hindawi.com/>, according to the following timetable.

Manuscript Due	April 1, 2008
First Round of Reviews	July 1, 2008
Publication Date	October 1, 2008

### Guest Editors

**Weidong Xiang**, University of Michigan, Dearborn, USA; [xwd@umich.edu](mailto:xwd@umich.edu)

**Javier Gozalvez**, University Miguel Hernández, Spain; [j.gozalvez@umh.es](mailto:j.gozalvez@umh.es)

**Zhisheng Niu**, Tsinghua University, China; [niuzhs@tsinghua.edu.cn](mailto:niuzhs@tsinghua.edu.cn)

**Onur Altintas**, Toyota InfoTechnology Center, Co. Ltd, Tokyo, Japan; [onur@jp.toyota-itc.com](mailto:onur@jp.toyota-itc.com)

**Eylem Ekici**, Ohio State University, USA; [ekici@ece.osu.edu](mailto:ekici@ece.osu.edu)

## Special Issue on Applications of Signal Processing Techniques to Bioinformatics, Genomics, and Proteomics

### Call for Papers

The recent development of high-throughput molecular genetics technologies has brought a major impact to bioinformatics, genomics, and proteomics. Classical signal processing techniques have found powerful applications in extracting and modeling the information provided by genomic and proteomic data. This special issue calls for contributions to modeling and processing of data arising in bioinformatics, genomics, and proteomics using signal processing techniques. Submissions are expected to address theoretical developments, computational aspects, or specific applications. However, all successful submissions are required to be technically solid and provide a good integration of theory with practical data.

Suitable topics for this special issue include but are not limited to:

- Time-frequency representations
- Spectral analysis
- Estimation and detection
- Stochastic modeling of gene regulatory networks
- Signal processing for microarray analysis
- Denoising of genomic data
- Data compression
- Pattern recognition
- Signal processing methods in sequence analysis
- Signal processing for proteomics

Authors should follow the EURASIP Journal on Bioinformatics and Systems Biology manuscript format described at the journal site <http://www.hindawi.com/journals/bsb/>. Prospective authors should submit an electronic copy of their complete manuscript through the EURASIP Journal on Bioinformatics and Systems Biology's Manuscript Tracking System at <http://mts.hindawi.com/>, according to the following timetable:

Manuscript Due	June 1, 2008
First Round of Reviews	September 1, 2008
Publication Date	December 1, 2008

### Guest Editors

**Erchin Serpedin**, Department of Electrical and Computer Engineering, Texas A&M University, College Station, TX 77843-3128, USA; [serpedin@ece.tamu.edu](mailto:serpedin@ece.tamu.edu)

**Javier Garcia-Frias**, Department of Electrical and Computer Engineering, University of Delaware, Newark, DE 19716-7501, USA; [jgarcia@ee.udel.edu](mailto:jgarcia@ee.udel.edu)

**Yufei Huang**, Department of Electrical and Computer Engineering, University of Texas at San-Antonio, TX 78249-2057, USA; [yhuang@utsa.edu](mailto:yhuang@utsa.edu)

**Ulisses Braga Neto**, Department of Electrical and Computer Engineering, Texas A&M University, College Station, TX 77843-3128, USA; [ulisses@ece.tamu.edu](mailto:ulisses@ece.tamu.edu)

# RESEARCH LETTERS IN COMMUNICATIONS

## Why publish in this journal?

**Research Letters in Communications** is devoted to very fast publication of short, high-quality manuscripts in the broad field of communications. The journal aims for a publication speed of 60 days from submission until final publication. Articles will be limited to a maximum of four published pages, and they should convey important results that have not been previously published.

### Why publish in this journal?

#### Wide Dissemination

All articles published in the journal are freely available online with no subscription or registration barriers. Every interested reader can download, print, read, and cite your article

#### Quick Publication

The journal employs an online «Manuscript Tracking System» which helps streamline and speed the peer review so all manuscripts receive fast and rigorous peer review. Accepted articles appear online as soon as they are accepted, and shortly after, the final published version is released online following a thorough in-house production process.

#### Professional Publishing Services

The journal provides professional copyediting, typesetting, graphics, editing, and reference validation to all accepted manuscripts.

#### Keeping Your Copyright

Authors retain the copyright of their manuscript, which are published using the “Creative Commons Attribution License,” which permits unrestricted use of all published material provided that it is properly cited.

#### Extensive Indexing

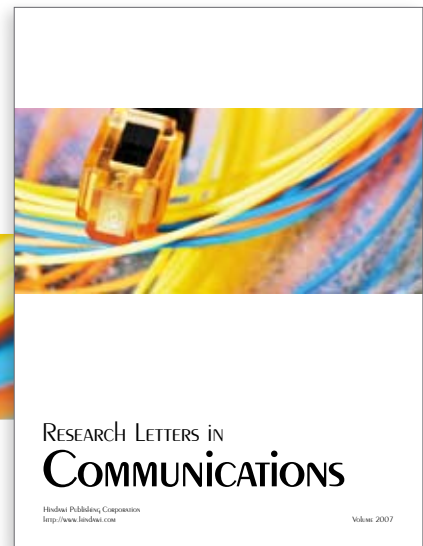
Articles published in this journal will be indexed in several major indexing databases to ensure the maximum possible visibility of each published article.

### Submit your Manuscript Now...

Please visit the journal’s website found at <http://www.hindawi.com/journals/rlc/> in order to submit your manuscript and click on the “Manuscript Submission” link in the navigational bar.

Should you need help or have any questions, please drop an email to the journal’s editorial office at [rlc@hindawi.com](mailto:rlc@hindawi.com)

ISSN: 1687-6741; e-ISSN: 1687-675X; doi:10.1155/RLC



#### Editor-in-Chief

Maria-Gabriella Di Benedetto  
*Italy*

#### Associate Editors

Huseyin Arslan  
*USA*

E. K. S. Au  
*Hong Kong*

Zhi Ning Chen  
*Singapore*

René Cumplido  
*Mexico*

Michele Elia  
*Italy*

Lijia Ge  
*China*

Amoakoh Gyasi-Agyei  
*Australia*

Peter Jung  
*Germany*

Thomas Kaiser  
*Germany*

Rajesh Khanna  
*India*

David I. Laurenson  
*UK*

Petri Mahonen  
*Germany*

Montse Najar  
*Spain*

Markus Rupp  
*Austria*

Nikos C. Sagiias  
*Greece*

Theodoros Tsiftsis  
*Greece*

Laura Vanzago  
*Italy*

Yang Xiao  
*USA*

Guosen Yue  
*USA*

Hindawi Publishing Corporation

410 Park Avenue, 15th Floor, #287 pmb, New York, NY 10022, USA

HINDAWI